Evidence of quasifission in the $^{16}O + ^{238}U$ reaction at sub-barrier energies

K. Banerjee,[1] T. K. Ghosh,[1] S. Bhattacharya,[1] C. Bhattacharya,[1] S. Kundu,[1] T. K. Rana,[1] G. Mukherjee,[1] J. K. Meena,[1] J. Sadhukhan,[1] S. Pal,[1] P. Bhattacharya,[2] K. S. Golda,[3] P. Sugathan,[3] and R. P. Singh[3]

[1]*Variable Energy Cyclotron Centre, 1/AF Bidhan Nagar, Kolkata 700 064, India*

[2]*Saha Institute of Nuclear Physics, 1/AF Bidhan Nagar, Kolkata 700 064, India*

[3]*Inter University Accelerator Centre, New Delhi 110 067, India*

(Received 22 September 2010; published 9 February 2011)

Mass distribution of fission fragments and neutron multiplicity in the $^{16}O + ^{238}U$ reaction were measured at near- and below-barrier energies. A sudden change in the fragment mass width, observed in the present measurement, confirmed the transition to quasifission at below-barrier energies; the same was indicated earlier from the study of fission fragment angular anisotropy. However, the present measurement of prescission neutron multiplicity as well as the earlier measurement of evaporation residue yield did not indicate any significant departure from the respective statistical model predictions throughout the energy range. It is argued that the first two probes are more sensitive for highly asymmetric systems, whereas all probes would be useful and complimentary to each other for study of quasifission in more symmetric systems, where quasifission is more dominant.

DOI: 10.1103/PhysRevC.83.024605 PACS number(s): 25.70.Jj, 25.70.Gh, 24.10.Pa

I. INTRODUCTION

Recently, there has been a lot of interest in the study of the mechanism of fusion reaction at near-barrier energies in the actinide region [1–5], which plays a key role in the synthesis of superheavy elements (SHEs). A major hindrance in the formation of superheavy elements is the suppression of the fusion-evaporation channel, not only by the equilibrium fission process but also by the nonequilibrium fission processes, such as quasifission (QF) and preequilibrium fission. In the case of quasifission, the dinuclear composite formed in the entrance channel directly undergoes fissionlike decay without going through the formation of a fully equilibrated compound nucleus. Thus, the occurrence of quasifission reduces the fusion (and hence the formation of SHE through subsequent evaporation) probability. So, the experimental challenges at present are to identify and, if possible, quantify the factors that hinder the compound nucleus formation (e.g., QF) and to locate the favorable conditions for fusion to occur.

However, identification of the reaction mechanism (particularly QF) is not always unambiguous. A very interesting case in point is the $^{16}O + ^{238}U$ system, which is a highly fissile, deformed system and therefore is a probable candidate for quasifission at near-barrier energies. Anomalous behavior of fission fragment angular anisotropy has been observed for this system at near-barrier energies, which indicates a significant contribution from noncompound nuclear fission. By assuming that the effect of quasifission is predominant in the sub-barrier region, where the orientation of the deformed target projectile system is crucial to determine the fusion trajectory, Hinde *et al.* [1] explained the anomalous energy dependence of the fragment anisotropy for the $^{16}O + ^{238}U$ system and concluded that there is a quasifission transition at sub-barrier energies. On the contrary, the cross sections of the evaporation residues (ERs) measured for the same system at near- and sub-barrier energies were reported to be consistent with the statistical theory [6], indicating that the contribution from noncompound fission (say, QF) is not significant. So, Nishio *et al.* [6] proposed that the observed anomalous fission fragment angular distribution may be due to the contribution from another competing mechanism, preequilibrium fission [7].

The distinction between quasifission and preequilibrium fission is, however, quite subtle. In preequilibrium fission, fusion and compound nucleus formation occur inside the true fission saddle point and thus fission takes place after the equilibration of all degrees of freedom except the K degree of freedom. This usually occurs in systems where the fission barrier height is comparable to the temperature and the fission width becomes sufficiently large that fission may take place before the system attains K equilibration, leading to larger fragment angular anisotropy. However, because mass equilibration is faster than shape equilibration, mass-equilibrated fragments may be reseparated as symmetric fission fragments in a preequilibrium fission reaction, before the system reaches spherical compound nuclear shape due to thermal diffusion. The effect of K nonequilibration diminishes with the decrease of temperature, so it is unexpected following the preequilibrium fission model [7] that angular anisotropy or fission mass width would increase with decreasing energies in the $^{16}O + ^{238}U$ system. On the contrary, in the case of quasifission, because the fission saddle point is more compact than the entrance channel contact configuration, the dinucleus, initially trapped in the conditional saddle point, evolves ultimately to reseparate before reaching mass symmetry. So, the study of fragment mass asymmetry in conjunction with other available probes is crucial to decipher the difference between the two processes.

Here we report a new, simultaneous measurement of fragment mass distribution and neutron multiplicity for the $^{16}O + ^{238}U$ system at near- and sub-barrier energies, which is extremely rarely, if ever, done. The effectiveness of mass distribution studies in elucidating the intricacies of the fusion-fission reaction mechanism has already been established [8]. Furthermore, prescission neutron multiplicity is also considered a useful probe for the study of fission dynamics. Because the time scales of quasifission (∼saddle-to-scission time) and fusion-fission (∼presaddle time + saddle-to-scission time) are

different, the appearance of quasifission at near-barrier energies should also be reflected in prescission neutron multiplicity data. Such change (decrease) in prescission neutron multiplicity with the onset of quasifission has been observed [9]. The present measurements are thus complimentary to the measurements made earlier for this system using different probes [1,6] and it is expected to shed new light on a long-standing controversy, the physics of which is still far from being fully understood experimentally as well as theoretically.

II. EXPERIMENT

The experiment was performed using a pulsed beam of ^{16}O obtained from 15UD Pelletron of the Inter University Accelerator Centre (IUAC), New Delhi. The targets used were ^{238}U of thickness 150 μg/cm^2 on 70 μg/cm^2 ^{12}C backing and self-supporting 400 μg/cm^2 ^{197}Au. The measurements on ^{16}O + ^{238}U were carried out at $E_{\rm lab} = 83$, 85, 87, 89, 92, 96, and 100 MeV. Measurements were also carried out on the ^{16}O + ^{197}Au system, which is a spherical projectile, deformed target ($\beta_2 = 0.113$) system, at an energy of 10 MeV above the Coulomb barrier, where only fusion-fission (FF) is expected for testing and calibration of the experimental setup and analysis procedures. For the detection of fission fragments, two large-area (20 cm × 6 cm) position-sensitive multiwire proportional counters (MWPCs) were placed at the folding angle for symmetric fission [10], at distances of 26 and 41 cm, respectively, from the center of the target on either side of the beam axis. Beam flux monitoring as well as normalization were performed using the elastic events collected by two silicon surface barrier detectors placed at ±10°. The event collection was triggered by the detection of a fission fragment in any of the MWPC detectors.

Four liquid-scintillator-based (BC501A) neutron detectors, each of dimension 5 in. × 5 in., were used for the detection of neutrons. The neutron detectors were placed outside the scattering chamber at angles 30°, 60°, 90°, and 120° with respect to the beam direction at a distance of 100 cm from the target. Thin flanges of 3-mm stainless steel were used in ports of the scattering chamber facing the neutron detectors to minimize the neutron scattering. The neutron detection thresholds were kept at 100 keVee by calibrating the detectors with a standard γ source. To keep the background of the neutron detector at a minimum level, the beam dump was kept 3 m away from the target and was well shielded with layers of lead and borated paraffin. Neutron energy was measured using the time-of-flight (TOF) technique, whereas the neutron γ discrimination was achieved by pulse shape discrimination and TOF. Neutron TOF was converted to neutron energy using a prompt γ peak in the TOF spectrum as a time reference. The efficiency correction for the neutron detector was performed using the Monte Carlo computer code NEFF [11]. The details of the neutron data analysis technique were reported earlier [12].

III. RESULTS

It is well known that at bombarding energy close to the Coulomb barrier, transfer fission (TF) is a dominant reaction channel. So, to extract the contributions of fusion-fission and

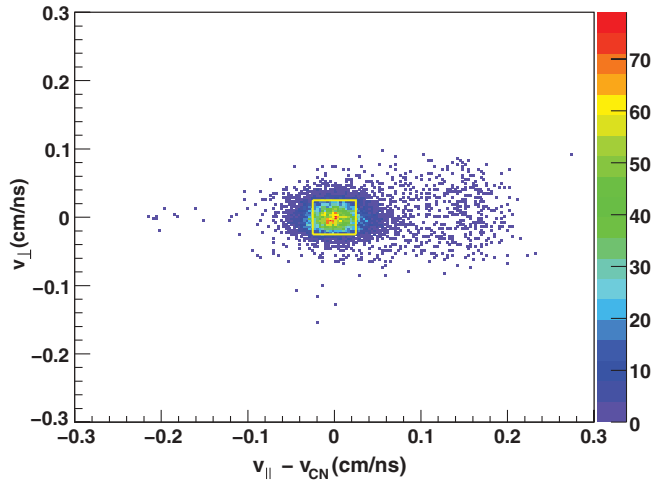

FIG. 1. (Color online) Measured distribution of velocity of the fissioning nuclei at $E_{\rm c.m.} = 81.5$ MeV. The (yellow) rectangle indicates the gate used to select the FF events.

quasifission, both of which are full momentum transfer processes, the TF contribution needs to be separated from experimental data [13]. The fission fragments from full momentum transfer events (FF and QF) were exclusively selected from the correlation of the velocity of the fissioning system ($v_\parallel$) in the beam direction relative to the recoil of the fused system and the velocity perpendicular to the reaction plane ($v_\perp$), as well as the correlation of the polar and azimuthal angles of the fragment (θ, ϕ) with respect to the beam axis. Figure 1 shows a typical fragment velocity distribution measured at $E_{\rm c.m.} =$ 81.5 MeV. For fusion-fission processes, the events were centered around the velocity coordinates (($v_\parallel$-$v_{\rm CN}$), $v_\perp$) = (0, 0).

A. Fission fragment mass distributions

The events corresponding to TF are scattered around nonzero ($v_\parallel$-$v_{\rm CN}$), $v_\perp$ values. The polar folding angle distribution of all fission events (FF and TF) is shown in Fig. 2, which

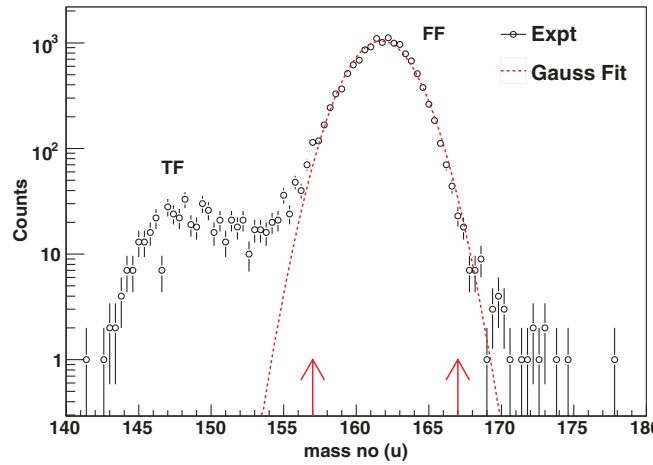

FIG. 2. (Color online) Measured folding angle distribution of all fission fragments in the reaction ^{16}O + ^{238}U at $E_{\rm c.m.} = 81.5$ MeV. The two arrows indicate the gate used to select the FF events for mass determination.

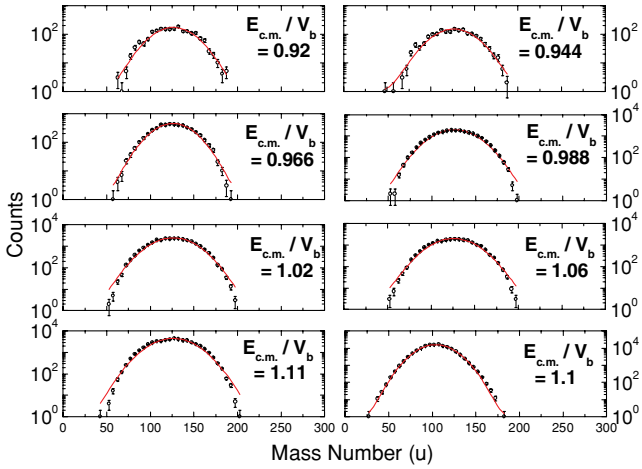

FIG. 3. (Color online) Measured mass distributions for the reactions $^{16}O + ^{238}U$ (excluding the bottom, right graph), and $^{16}O + ^{197}Au$ (bottom, right) at energies near and above the Coulomb barrier. The Gaussian fits are shown by solid (red) lines.

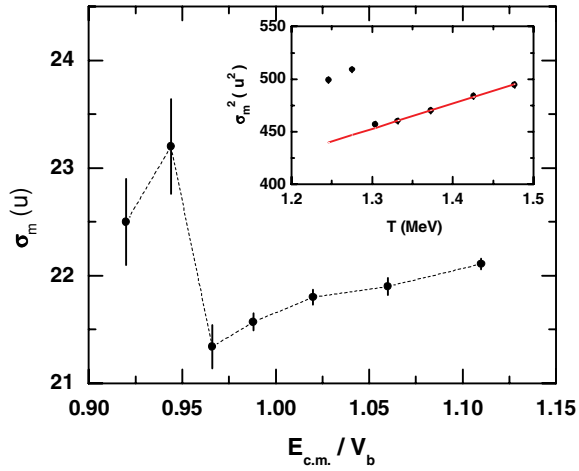

FIG. 4. (Color online) Variation of σ_m as a function of $E_{\text{c.m.}}/V_b$; the dotted curve is a visual guide only. Inset shows the variation of σ_m^2 with T (MeV), along with a linear fit to the data [solid (red) line].

shows that the measured folding angle distribution of FF events peaks around 165°, which is consistent with the expected value for full momentum transfer events. The events for the TF peak around a smaller folding angle as the ejectile moves in the backward direction. The fission fragments are well separated from elastic and quasielastic reaction channels, as far as the time correlation and energy loss spectra are concerned. The fragment masses were determined from the difference of the time of flight, polar and azimuthal angles, momentum, and recoil velocities for each event [14]. Representative mass distributions, near and above the Coulomb barrier energies, are shown in Fig. 3 for the $^{16}O + ^{238}U$ and $^{16}O + ^{197}Au$ system. It is observed that measured mass distributions are well fitted with a single Gaussian distribution at all energies.

The variation of the standard deviation (σ_m) of the fitted Gaussian to the experimental fission fragment mass distribution as a function of $E_{\text{c.m.}}/V_b$, where $E_{\text{c.m.}}$ is the incident energy in center of mass and V_b is the Coulomb barrier, is shown in Fig. 4. It is seen that there is a sudden increase in σ_m as energy decreases to below-barrier energies. Since the TF contribution has been removed as explained above, the increase in width of the mass distribution is a clear indication of a sudden qualitative change in the degree of mass equilibration in the $^{16}O + ^{238}U$ system at below-barrier energies. Assuming that the sudden change in the degree of mass equilibration (and vis-á-vis σ_m) is due to the onset of quasifission, it may be possible to extract the contribution of quasifission in the total fission process in the following way. At above-barrier energies, variances of mass distribution are only due to fusion-fission and they follow the relation $\sigma_m^2 = (\sigma_m^2)^{\text{FF}} \propto T$, where $T = \sqrt{E^*/a}$ is the nuclear temperature, E^* is the excitation energy at the scission point, $a = A_{\text{CN}}/10$ is the level density parameter, and A_{CN} is the compound nucleus mass number. The values of $(\sigma_m^2)^{\text{FF}}$ at below-barrier energies are then extracted by extrapolating the σ_m^2 values at above-barrier energies to lower energies using linear curve fitting (Fig. 4). The percentage of QF can then be estimated by comparing the areas under the Gaussians having variances σ_m and $(\sigma_m)^{\text{FF}}$. It is found that the QF contribution at two below-barrier energies are ∼6% (at 85 MeV) and ∼5% (at 83 MeV).

B. Neutron multiplicities

Assuming that the neutrons are emitted from thermally equilibrated sources, the prescission and postscission components of the neutron spectrum have been extracted from the experimental neutron energy distribution using a phenomenological moving source model. Three moving sources were taken into consideration; the prescission neutrons were assumed to be emitted from a compound nuclear source and the postscission neutrons were assumed to be emitted from either of the two fully accelerated fission fragments. Optimum source parameters were extracted by fitting the data with three source distribution functions given below, through the χ-square minimization technique [15]:

$$\frac{d^2M_n^{\text{tot}}}{dE_n d\Omega} = \sum_{i=1}^{3} \frac{M_n^i \sqrt{E_n})}{2(\pi T_i)^{3/2}} \times \exp\left(- \frac{E_n - 2\sqrt{E_n E_i/A_i}\cos\theta_i + E_i/A_i}{T_i} \right), \quad (1)$$

where E_n is the laboratory energy of the neutron and E_i, T_i, and M_n^i are the energy, temperature, and multiplicity of ith neutron emission source (where $i = 1, 2, 3$ corresponds to the prescission and two postscission sources). A_i is the mass of the ith neutron source and θ_i represent the relative angle between the neutron direction and the source direction. In this analysis, TF events were precisely removed by considering suitable gates as mentioned above. The total neutron multiplicity, M_n^{tot}, was estimated as $M_n^{\text{tot}} = M_n^{\text{pre}} + 2M_n^{\text{post}}$. Figure 5 shows the neutron energy spectra along with fits for pre- and postscission contributions.

The prescission, postscission, and total neutron multiplicities per fission as a function of $E_{\text{c.m.}}/V_b$, where V_b is the

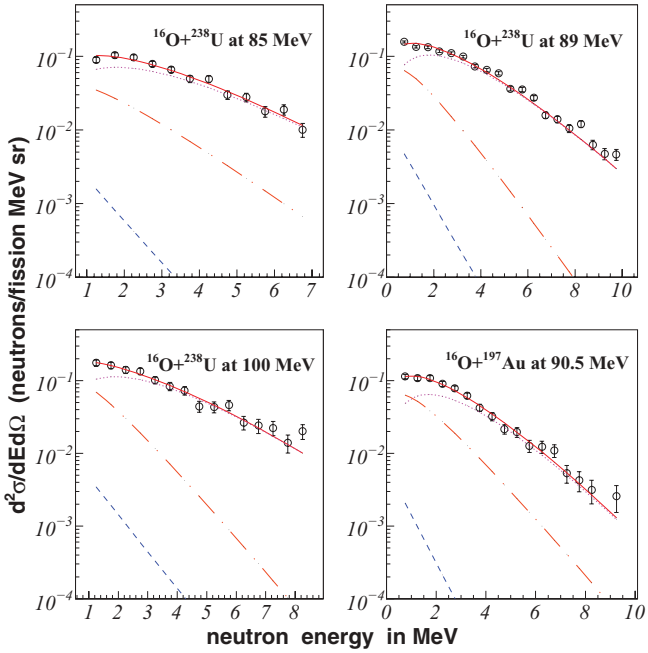

FIG. 5. (Color online) Measured neutron multiplicity spectra (open circles) along with the fits for the prescission [dot-dashed (brown) curve] and postscission components from the two fission fragments [dotted (magenta) and dashed (blue) curves]. The solid (red) curve represents total contribution.

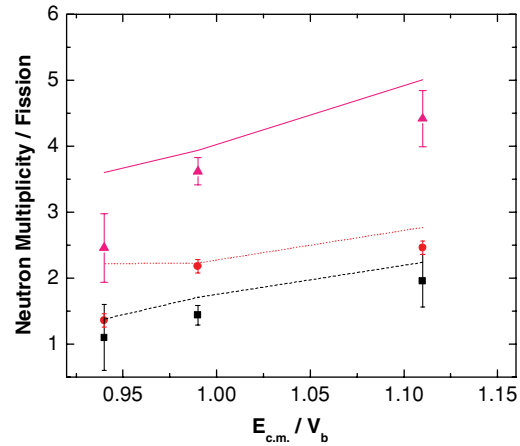

FIG. 6. (Color online) Comparison of experimental $M_n^{\rm pre}$ (squares), $M_n^{\rm post}$ (circles) and $M_n^{\rm total}$ (triangles) with respective theoretical estimates [dotted (black), dashed (red), and solid (pink) curves] at different energies.

barrier energy, are shown in Fig. 6 along with the respective statistical model [16] predictions, where the Kramer fission width was compared with neutron, proton, and α- and γ-ray evaporation widths using the Monte Carlo technique. The experimental fusion cross sections were taken from Ref. [6]. The value of the friction coefficient β for the present calculation was taken to be 10×10^{-21} s^{-1} for all excitation energies. The measured fission fragment mass distribution was used in the calculation to estimate the postscission neutron emission. The calculated $M_n^{\rm pre}$ values are found to be in good agreement with experimentally estimated values; the calulated $M_n^{\rm post}$ values are also found to be in fair agreement with corresponding experimental estimates except at below-barrier energy ($E_{\rm lab} = 85$ MeV). This discrepancy at below-barrier energy, in particular, may be due to noninclusion of the shell correction in the fission barrier used in the present calculation; inclusion of the shell correction usually increases the fission barrier [17] and thereby reduces the excitation energy of the fragments.

IV. DISCUSSION

It is interesting to note that the present mass distribution result clearly shows a sharp change in the mass distribution width, which is a signature of a sudden qualitative change in the degree of mass equilibration; this may be considered strong evidence for onset of quasifission in the ^{16}O + ^{238}U system at below-barrier energies. This thus reaffirms the observation made earlier about the onset of quasifission at below-barrier energies for the same system from the study of fission fragment angular anisotropy measurement [1]. On the contrary, the present measurement of prescission neutron multiplicity for the same system at above- and below-barrier energies is clearly consistent with the standard statistical model [16] prediction; this apparently indicates that quasifission does not significantly modify the complete fusion yield (and vis-á-vis $M_n^{\rm pre}$) for this system even at below-barrier energies. A similar inference was drawn from the study of ER measurements for the same system [6], where, too, no departure from statistical model prediction was seen, and it was concluded that the anomalous fragment anisotropy might be linked to preequilibrium fission, not quasifission.

The apparent inconsistency in the inferences being drawn about the onset of QF from four different probes (fragment angular anisotropy and fragment mass distribution width on one hand, and evaporation residue cross section and prescission neutron multiplicity on the other hand) warrants some discussion at this point. Because two different probes (fragment angular anisotropy and fragment mass distribution width) have shown clear signatures of a transition to QF for this system at below-barrier energies, we can conclude that quasifission transition is "confirmed" for the ^{16}O + ^{238}U system at below-barrier energies. Although fragment angular anisotropy may be common to both preequilibrium fission and quasifission, the observation of the change in fragment mass width, which is linked with nonequilibration of the mass asymmetry degree of freedom, confirms the onset of quasifission. Moreover, because the temperature of the system, as extracted from the present neutron data, is $\sim$1 MeV and the shell-corrected barrier is 6.24 MeV [17], preequilibrium fission may be less dominant than expected at these energies [7]. In addition, because the value of ($Z_{\rm proj}Z_{\rm target}$) is very low (736) for this system, the fusion hindrance due to the Coulomb factor (extra push) may not be significant; therefore, it may be inferred that the origin of quasifission in the ^{16}O + ^{238}U system at below-barrier energies is primarily due to the orientation of the deformed target projectile system.

That the other two probes (ER and prescission neutron multiplicity) did not show unambiguous signatures of

quasifission transition for this system in particular may be intutively understood in the following way. The ER measurement is more sensitive for more symmetric systems ($Z_{\rm proj}Z_{\rm target} \gtrsim$ 1500–1600), for which the quasifission fraction is comparable or even larger than that of fusion-fission. This was established in a recent study of ER measurement for the $^{34}S + ^{238}U$ system at near-barrier energies [18], where significant reduction in ER formation was observed. On the contrary, in the case of the highly asymmetric $^{16}O + ^{238}U$ ($Z_{\rm proj}Z_{\rm target} = 736$) system, the present experimental estimate of quasifission (∼5%–6%) is much smaller than the fusion-fission cross section. The present experimental estimates are also close to the geometrical estimate (∼13%) of the orientation-dependent quasifission (tip collision) [6] for the same system. Hence, the change in ER cross section may not be appreciable to be detected unambiguously. The same argument holds for prescission neutron multiplicity as well. However, for the present system, which is highly asymmetric, no departure of $M_n^{\rm pre}$ from statistical model prediction indicating transition to quasifission was seen; for a more symmetric system ($^{58,64}Ni + ^{208}Pb$), such a change in $M_n^{\rm pre}$ indicating quasifission has already been reported in the literature [9].

V. SUMMARY AND CONCLUSION

To conclude, the present observation of the sudden change in fragment mass distribution width along with the earlier observation of anomalous fragment angular anisotropy confirm the onset of quasifission of the $^{16}O + ^{238}U$ system at below-barrier energies. However, the present measurement of prescission neutron multiplicity as well as the earlier measurement of evaporation residue yield do not show any departure from standard statistical model predictions. This may be due to the insensitivity of these two probes for highly asymmetric system with low $Z_{\rm proj}Z_{\rm target}$ (≪1500–1600) value; for a more symmetric system with higher $Z_{\rm proj}Z_{\rm target}$ value, where the QF fraction is comparable to fusion-fission, both $M_n^{\rm pre}$ and ER yield may also be equally useful for such studies.

ACKNOWLEDGMENTS

We are thankful to Dr. S. K. Das for providing help in making the target. We are also thankful to the IUAC Pelletron staff for providing the high-quality pulsed beam.

[1] D. J. Hinde, M. Dasgupta, J. R. Leigh, J. P. Lestone, J. C. Mein, C. R. Morton, J. O. Newton, and H. Timmers, Phys. Rev. Lett. **74**, 1295 (1995).
[2] T. K. Ghosh *et al.*, Phys. Rev. C **79**, 054607 (2009).
[3] R. Rafiei, R. G. Thomas, D. J. Hinde, M. Dasgupta, C. R. Morton, L. R. Gasques, M. L. Brown, and M. D. Rodriguez, Phys. Rev. C **77**, 024606 (2008).
[4] M. G. Itkis *et al.*, Nucl. Phys. A **734**, 136 (2004).
[5] K. Nishio, H. Ikezoe, S. Mitsuoka, I. Nishinaka, Y. Nagame, Y. Watanabe, T. Ohtsuki, K. Hirose, and S. Hofmann, Phys. Rev. C **77**, 064607 (2008).
[6] K. Nishio, H. Ikezoe, Y. Nagame, M. Asai, K. Tsukada, S. Mitsuoka, K. Tsuruta, K. Satou, C. J. Lin, and T. Ohsawa, Phys. Rev. Lett. **93**, 162701 (2004).
[7] V. S. Ramamurthy and S. S. Kapoor, Phys. Rev. Lett. **54**, 178 (1985).
[8] T. K. Ghosh, S. Pal, T. Sinha, S. Chattopadhyay, P. Bhattacharya, D. C. Biswas, and K. S. Golda, Phys. Rev. C **70**, 011604(R) (2004); T. K. Ghosh, S. Pal, K. S. Golda, and P. Bhattacharya, Phys. Lett. B **627**, 26 (2005).
[9] L. Donadille *et al.*, Nucl. Phys. A **656**, 259 (1999).
[10] V. E. Viola, K. Kwiatkowski, and M. Walker, Phys. Rev. C **31**, 1550 (1985).
[11] G. Dietze and H. Klein, PTB-ND-22 Report, 1982.
[12] K. Banerjee *et al.*, Nucl. Instrum. Methods Phys. Res. A **608**, 440 (2009).
[13] N. Majumdar, P. Bhattacharya, D. C. Biswas, R. K. Choudhury, D. M. Nadkarni, and A. Saxena, Phys. Rev. C **51**, 3109 (1995).
[14] T. K. Ghosh, S. Pal, T. Sinha, S. Chattopadhyay, K. S. Golda, and P. Bhattacharya, Nucl. Instrum. Methods Phys. Res. A **540**, 285 (2005).
[15] H. Rossner, D. Hilscher, D. J. Hinde, B. Gebauer, M. Lehmann, M. Wilpert, and E. Mordhorst, Phys. Rev. C **40**, 2629 (1989).
[16] J. Sadhukhan and S. Pal, Phys. Rev. C **78**, 011603 (2008); **79**, 019901(E) (2009).
[17] P. Moller, A. J. Sierk, T. Ichikawa, A. Iwamoto, R. Bengtsson, H. Uhrenholt, and S. Aberg, Phys. Rev. C **79**, 064304 (2009).
[18] K. Nishio *et al.*, Phys. Rev. C **82**, 024611 (2010).